



## Modulation of protein release from photocrosslinked networks by gelatin microparticles

Ashley A. Weiner, Marc C. Moore, Amanda H. Walker, V. Prasad Shastri\*

Department of Biomedical Engineering, Vanderbilt University, 5824 Stevenson Center, Nashville, TN 37232, USA

### ARTICLE INFO

#### Article history:

Received 5 November 2007

Received in revised form 11 March 2008

Accepted 15 April 2008

Available online 2 May 2008

#### Keywords:

Polyanhydrides

Cyclodextrin

Controlled dual release

Bone augmentation

### ABSTRACT

Injectable delivery systems are attractive as vehicles for localized delivery of therapeutics especially in the context of regenerative medicine. In this study, photocrosslinked polyanhydride (PA) networks were modified by incorporation of microparticles to modulate long-term delivery of macromolecules. The *in vitro* release of two model proteins (horseradish peroxidase (HRP) and bovine serum albumin labeled with fluorescein isothiocyanate (FITC-BSA)) were evaluated from networks composed of sebacic acid dimethacrylate (MSA), 1,6-bis-carboxyphenoxyhexane dimethacrylate (MCPH), poly(ethylene glycol) diacrylate (PEGDA), and calcium carbonate ( $\text{CaCO}_3$ ), supplemented with gelatin microparticles or sodium chloride crystals. Prior to incorporation into the networks, proteins were formulated into granules by dilution with a cyclodextrin excipient and gelatin-based wet-granulation. Protein release was modulated by incorporation of microparticles into photocrosslinked PA networks, presumably by enabling aqueous channels through the matrix. Furthermore, a dual release system has been demonstrated by incorporation of protein in both the PA matrix and the gelatin microparticles. These results suggest that microparticle incorporation into the photocrosslinked PA system may be a useful strategy to modulate protein release in injectable delivery systems for the long-term delivery of macromolecules. These composites present an interesting class of materials for bone regeneration applications.

© 2008 Elsevier B.V. All rights reserved.

### 1. Introduction

In the recent past, our laboratory efforts have focused on the exploration of the photocrosslinked polyanhydride (PA) system as a scaffold for hard tissue regeneration and drug delivery. This system is based on anhydride monomers with reactive methacrylate functionalities and has been developed for use in orthopedic tissue repair and regeneration (Anseth et al., 1999; Burkoth et al., 2000; Muggli et al., 1999). Upon exposure to light radiation, this system can be rapidly crosslinked *in situ* into a high strength degradable network. This system has several advantages over traditional PLGA systems for drug delivery. First, as a result of the anhydride linkages, PA based systems are capable of undergoing surface erosion (Tamada and Langer, 1993) and achieving predictable near-zero order drug release (Determan et al., 2004). Additionally, the capability of *in situ* formation is of particular importance in tissue engineering (TE) applications in which physical conformation of the device to an implant site is an important prerequisite for optimal tissue healing (Shastri et al., 1999).

We have shown that a traditional photocrosslinked PA system composed of 1,6-bis-carboxyphenoxyhexane dimethacrylate (MCPH) and sebacic acid dimethacrylate (MSA) can be easily modified with additives such as  $\text{CaCO}_3$  and PEGDA to modulate degradation properties such as mass loss, water uptake, pH and mechanical strength while providing no adverse effects on the crosslinking capabilities of the system (Weiner et al., 2007). Additionally, we have demonstrated that this system possesses a robust capability for long-term delivery of macromolecules (Weiner et al., 2008). We have implemented a protein stabilization strategy previously developed in our laboratory to protect proteins from free radicals during polymerization (Baroli et al., 2003), with some minor modifications to stabilize and disperse the protein in the PA system developed for the spinal fusion application. Using these strategies, we have demonstrated that the photocrosslinked PA system can serve as an injectable vehicle for the long-term delivery of active proteins. Although most studies of the photocrosslinked PA system have focused on orthopedic applications, a more general application would involve intra-muscular and sub-dermal injectable systems capable of long-term delivery of macromolecules.

In our previous work, we were able to achieve long-term (over 4 months) release of enzymatically active protein (horseradish peroxidase (HRP)), although relatively low levels of protein release

\* Corresponding author. Tel.: +1 615 322 8005; fax: +1 615 343 7919.

E-mail addresses: [prasad.shastri@vanderbilt.edu](mailto:prasad.shastri@vanderbilt.edu), [prasad.shastri@gmail.com](mailto:prasad.shastri@gmail.com) (V.P. Shastri).

were attained. The release rate and profile were modestly modulated by altering matrix hydrophobicity (MCPH:MSA ratio or PEGDA content). Significant modulation of protein release rates and profiles is difficult in this photocrosslinked system outside of altering matrix hydrophobicity. Although reactive and nonreactive additives can be incorporated with ease, an upper limit exists after which crosslinking and/or structural integrity of the system is impaired.

One proposed driving force for protein release (in addition to degradation) is protein diffusion through aqueous channels in the wetted network (Saltzman and Langer, 1989). Maximization of the channel volume within the matrix by incorporation of porogens would be one mechanism for increasing release. One possible methodology for induction of microscale channels is the incorporation of microparticles or salt crystals within the crosslinked matrix (Hedberg et al., 2005). In the field of TE, microparticles alone suffer limitations, since they do not provide a substrate for cellular or tissue ingrowth. However, diverse uses for incorporation of microparticles into TE scaffolds have been identified. Initially, leachable porogens such as microparticles of gelatin (Draghi et al., 2005) or NaCl (Liao et al., 2002) have been used to generate porosity in scaffolds by solvent casting or particulate leaching. More recently, drug or protein-loaded microparticles have been incorporated into TE scaffolds (such as polypropylene fumarate (Hedberg et al., 2005) or oligo(poly(ethylene glycol) fumarate) (Holland et al., 2005)) to form composites with the capability of delivering bioactive molecules that aid in tissue regeneration. For these drug delivery applications, biodegradable microparticles composed of gelatin (Muvaffak et al., 2004), co-polymers of lactic acid and glycolic acid (PLGA) (Hedberg et al., 2005), or PAs (Determan et al., 2004) have garnered much interest.

In the current study, two model proteins (HRP and FITC-BSA) were selected for release from porous photocrosslinked PA networks. The current strategies employed include both particulate leaching of NaCl and gelatin microparticles as well as release of protein from composites composed of protein-loaded gelatin microparticles within photocrosslinked PA networks (see Fig. 1). This study is the first to evaluate the incorporation of porogens in the photocrosslinked PA system. In addition, it is the first to employ the particulate leaching strategy as a primary means of facilitating protein release. The overall objective of this study was therefore to demonstrate the ease of modulation of this system for improving delivery of peptides and proteins. Specifically, we aim to answer the following questions: (1) can delivery of macromolecules be controlled by incorporation of porogens (NaCl and gelatin microparticles) within the matrix? (2) Can the protein carrier affect protein release? and (3) Does the physicochemical nature of the macromolecule affect release? By answering these questions, we have expanded on our previous studies to demonstrate versatility in release profiles from the photocrosslinked PA system for the long-term delivery of active macromolecules.

## 2. Experimental

### 2.1. Materials

Methacrylic acid, sebacoyl chloride, triethylamine, methylene chloride, sodium bicarbonate, sodium sulfate, 4-hydroxybenzoic acid, 1,6-dibromohexane, methacryloyl chloride, poly(ethylene glycol) diacrylate (PEGDA), camphorquinone (CQ), ethyl 4-(dimethylamino)benzoate (4-EDMAB), benzoyl peroxide (BPO), dimethyl toluidine (DMT), *n*-methyl pyrrolidone (NMP), bovine serum albumin fluorescein isothiocyanate conjugate (FITC-BSA), calcium carbonate (CaCO<sub>3</sub>), bovine gelatin B, and glutaraldehyde were obtained from Sigma–Aldrich. HRP, 3,3',5,5'-

tetramethylbenzidine (TMB) substrate kits and Coomassie-based Bradford assay kits were purchased from Pierce. All materials were used as received.

### 2.2. Monomer synthesis

Monomers were synthesized as previously described (Weiner et al., 2007). In brief, MSA was synthesized by a substitution reaction of a diacid dichloride with an acid (sebacoyl chloride and methacrylic acid). 1,6-Bis-carboxyphenoxyhexane (CPH) was synthesized by substitution of an alkyl dihalide with an acid (1,6-dibromohexane and 4-hydroxybenzoic acid). MCPH was synthesized by transesterification of CPH with methacryloyl chloride.

### 2.3. Protein formulation

HRP and FITC-BSA were used as model proteins. The formulation for incorporation into photocrosslinked polyanhydride matrices was based on methods described by Baroli et al. (2003). In brief, each protein (P) was first pulverized by trituration in a Teflon dish with a Teflon-coated spatula. Pulverized protein was then mixed with hydroxypropyl- $\beta$ -cyclodextrin (HP $\beta$ CD), in a ratio 1:50 (FITC-BSA) or 1:100 (HRP) w/w (P:HP $\beta$ CD), by geometric dilutions until a homogeneous powder was obtained. Subsequently, this P-HP $\beta$ CD mixture was granulated with a 5% aqueous solution of gelatin B (100 mg of gelatin solution per 1 g of P-HP $\beta$ CD mixture) to produce a slightly wet mass, which was then forced through a 250- $\mu$ m sieve to yield granules. The granulated P-HP $\beta$ CD mixture was stored at -20 °C and analyzed for fluorescence (FITC-BSA) or enzymatic activity (HRP) prior to use.

To verify the homogeneity of the protein distribution in freshly prepared powders, a content uniformity test was used. Prior to granulation, the P-HP $\beta$ CD mixtures were sampled uniformly over their entirety without mixing. Using a sample size of 10 mg ( $n = 10$  per each formulation), the mixtures were then quantified for protein content using a Coomassie-based Bradford Assay. For each set of 10 samples, the mean and the standard deviation was calculated. Requirements of the test were considered met if the amount of protein was within the limits of 85 and 115% of the expected values, and the relative standard deviation (expressed as a percentage) was less than or equal to 6%.

### 2.4. Preparation of gelatin microparticles

Gelatin microparticles were fabricated as described by Holland et al. (2005). Briefly, 5 g of basic gelatin was dissolved in 45 ml of deionized water by heating to 60 °C under constant stirring. The aqueous gelatin solution was added dropwise via a syringe and 21-G needle to 250 ml of olive oil while maintaining a stirring rate of 500 rpm. Stirring was maintained while the emulsion temperature was decreased to 15 °C to induce gelation. After 30 min, 100 ml of chilled acetone were added. The microparticles were removed by vacuum filtration and were washed four times with acetone to remove residual olive oil. Microparticles were sized by passing through sieves of sizes ranging from 500 to 106  $\mu$ m.

### 2.5. Crosslinking of gelatin microparticles

Gelatin microparticles were crosslinked by stirring in a 0.1% solution of Tween 80 containing 0.5% glutaraldehyde for 12 h at 15 °C. Crosslinked microparticles were collected by vacuum filtration. The microparticles were washed in deionized water and then incubated in a 25-mM glycine solution for 1 h to block any unreacted glutaraldehyde. The microparticles were collected by vacuum, washed in deionized water, and vacuum-dried overnight.

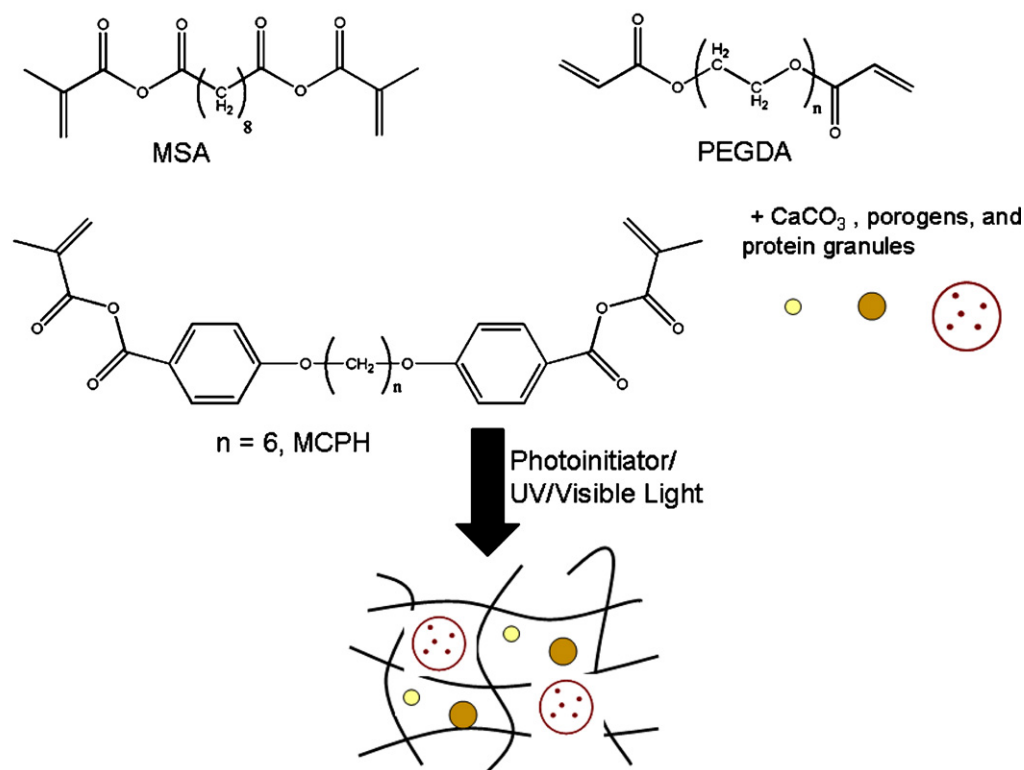


**Fig. 1.** Schematic of photocrosslinking. Anhydride monomers (MSA, MCPH), PEGDA, CaCO<sub>3</sub> and protein granules were mixed to form a paste. Mixtures were photocrosslinked after addition of photoinitiators and exposure to visible light.

Crosslinked microparticles were then sized by passing through a gradient of sieves.

## 2.6. Protein loading of crosslinked gelatin microparticles

Solutions of protein in phosphate buffered saline were prepared for loading of the crosslinked gelatin microparticles. Microparticle loading was achieved by incubating 5  $\mu$ l of protein solution (2 mg/ml, HRP or FITC-BSA) per mg of gelatin microparticles. This solution volume was significantly below the theoretical equilibrium swelling volume of the microparticles, ensuring complete protein adsorption by the particles. The microparticle-protein mixture was vortexed completely and incubated overnight at 4 °C to allow adsorption to occur.

## 2.7. In vitro protein release from crosslinked gelatin microparticles

HRP and FITC-BSA release from crosslinked gelatin microparticles was assessed in PBS. Loaded microparticle were weighed and incubated with 1 ml of PBS. All specimens were incubated at 37 °C with shaking (60 rpm). At predetermined timepoints, the specimens were pelleted by centrifugation. The release buffer was removed and replaced with fresh PBS. The presence of protein in the release buffer was quantified by correlation with a standard curve (see assays for HRP and FITC-BSA below). Protein release was quantified by calculating the cumulative protein release and normalizing to the total loaded protein in each specimen as a percentage.

## 2.8. Sample preparation and photopolymerization

Photopolymerizations were initiated with a dual initiator strategy, composed of CQ/4-EDMAB for light-initiated crosslinking, and

BPO/DMT for chemically initiated crosslinking, as previously developed and described (Weiner et al., 2007). Sample formulations were prepared by thoroughly mixing the anhydride monomers (MCPH and MSA), the additives (PEGDA and CaCO<sub>3</sub>), and formulated protein in appropriate amounts. The PEGDA and CaCO<sub>3</sub> amounts were 10% of the mass prior to adding the microparticles. In addition, the appropriate porogen (NaCl or gelatin microparticles) was added and mixed until a uniform paste was achieved. An appropriate quantity of a BPO/CQ in NMP and 4-EDMAB/DMT in NMP was added to yield a final quantity of up to 0.1 wt% for each of CQ, BPO, 4-EDMAB, and DMT in the formulation. Uniform discs (4 mm in height and 9 mm in diameter) were prepared in Teflon molds. Samples were polymerized with a blue dental lamp (CuringLight XL1500).

## 2.9. In vitro release studies

*In vitro* protein release was assessed in phosphate buffered saline, pH 7.4 at 37 °C to mimic physiological conditions. Samples were maintained at 60 rpm on an orbital shaker throughout degradation studies. The discs were degraded in 10 ml of buffer. Buffer was replaced at predetermined timepoints for entire duration of the study to minimize the effects protein deactivation in solution and to maintain sink conditions for degradation. The samples of buffer were analyzed for the presence of HRP (activity assay) or FITC-BSA (fluorescence) as appropriate.

## 2.10. HRP activity assay

Enzymatic activity of HRP was calculated by quantification of oxidized TMB substrate in a peroxide solution using a TMB Substrate Kit. Serial dilutions of HRP release buffer were performed in PBS. 100  $\mu$ l of each appropriate dilution was added to a 96-well plate. Using a multichannel pipettor, 100  $\mu$ l of TMB substrate

in a peroxidase buffer was added and the plate was immediately transferred to a plate reader for analysis. The concentration of the oxidized product was measured every 5 min for 30 min total at 462 nm on a BioTek II microplate reader. HRP concentrations in release buffer were compared to freshly prepared HRP standards ranging from 0.01 to 1 mU/ml. The linear range for a 30-min incubation was between 0.01 and 0.25 mU/ml. The detection limit was 0.01 mU/ml.

### 2.11. Quantification of FITC-BSA fluorescence

Concentration of FITC-BSA was quantified by fluorescence at 488 nm on a BioTek II microplate reader. 200  $\mu$ l FITC-BSA containing release buffer was loaded in wells of a 96-well plate. FITC-BSA concentrations were compared to freshly prepared standards ranging from 0.01 to 2  $\mu$ g/ml. The detection limit for the assay was 0.01  $\mu$ g/ml.

### 2.12. Scanning electron microscopy

Dried PA samples were cryo-fractured by cooling in liquid nitrogen and the cross-section was analyzed using scanning electron microscopy (SEM). The pellets were sputter-coated with gold-palladium to minimize charging and then mounted onto aluminum stubs using conductive tape for imaging. SEM images were obtained using a Hitachi S-4200 SEM at an acceleration voltage of 5 keV.

### 2.13. Statistical analysis

All release data is presented as a percentage of total loaded protein. Statistical analysis for comparison of burst release, cumulative release, and rates of release was performed using a Student's *t*-test with a minimum confidence level of 0.05 for statistical significance. All experiments were performed with  $n = 3-5$  and are reported as mean  $\pm$  standard deviation of the mean.

## 3. Results

### 3.1. HRP release from photocrosslinked PA matrices with NaCl or gelatin microparticle-induced porosity

Although previous experimentation in our laboratory demonstrated capability of delivering active proteins over a long timeframe at a tunable rate, the cumulative HRP release was less than 20% of total loaded HRP after 35 days. We therefore hypothesized that the introduction of water-soluble porogens such as NaCl or crosslinked gelatin microparticles might accelerate the release of HRP (see formulations in Table 1a). The most hydrophobic net-

**Table 1**

Experimental design for evaluation of microparticle leaching for modulation of protein release

MCPH:MSA ratio	Granulated protein	Microparticle loading	Microparticle size ( $\mu$ m)	Microparticle type
a				
70:30	HRP	25 w/w%	<106	NaCl
70:30	HRP	25 w/w%	250	Gelatin B
b				
70:30	HRP	75 v/v%	180–250	Gelatin B
70:30	HRP	75 v/v%	250–300	Gelatin B
c				
70:30	HRP	33 v/v%	106–180	Gelatin B
70:30	HRP	55 v/v%	180–250	Gelatin B
30:70	HRP	33 v/v%	180–250	Gelatin B
30:70	HRP	55 v/v%	106–180	Gelatin B

work system composed of MCPH:MSA in 70:30 ratio supplemented with 10% of PEGDA and CaCO<sub>3</sub> was selected, as it resulted in the slowest protein release in unmodified systems and furthermore, based on our previous assessments of degradation this system minimized water uptake and afforded maintenance of sample integrity throughout experimental timeframes. In Fig. 2, the surface and a cross-section of a gelatin microparticle loaded network can be seen. HRP release was measured by activity assay in which TMB substrate was oxidized in the presence of a peroxide buffer. As a result, only active release protein was detected. Introduction of 25 w/w% of 250  $\mu$ m gelatin microspheres into the system resulted in the release of 56% of loaded HRP over a 5-week period which represents a fivefold increase over the 10% release seen in the unmodified system. A significant increase in protein release was seen both during the 24 h burst release ( $p = 0.001$ ) as well as during the long-term release phase (days 7–35,  $p = 0.005$ ) in the gelatin microparticle supplemented system. However, when NaCl particles (<106  $\mu$ m) were incorporated into networks as a porogen, no difference in release rate occurred in comparison with the unmodified, nonporous matrix. Fig. 3 shows the release profiles over 35 days for these three formulations. In addition, Table 2 compares the 24 h burst effect release, the cumulative release after 48 h, the long-term release rate (between days 7 and 35), and the total cumulative release for the unmodified, nonporous network, and for the network containing 250  $\mu$ m gelatin microparticles. There was a statistically significant difference for all calculated parameters in this table. However, when comparing the unmodified, nonporous network to the network containing <106  $\mu$ m NaCl crystals (Fig. 3B), the only significant difference occurred in the burst release phase. Since 250  $\mu$ m diameter salt crystals were not readily available from commercial sources and, furthermore, since crushing larger salt crystals failed to yield crystals in this size range in a reproducible

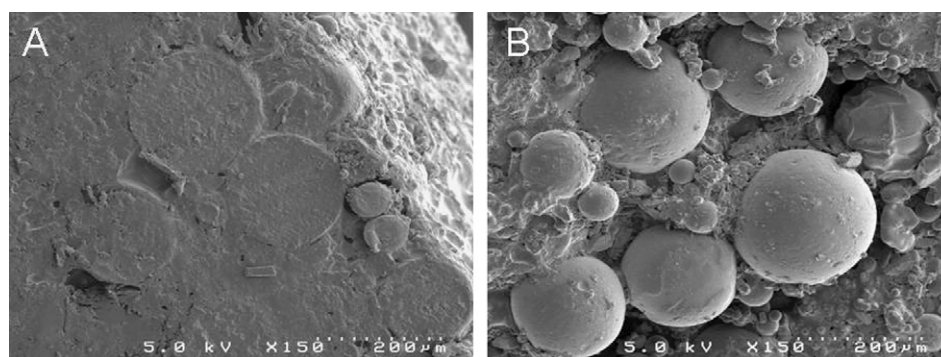


**Fig. 2.** SEM images of gelatin microparticle-PA network composites. (A) Cryo-section through center of crosslinked matrix. (B) Surface of crosslinked matrix.



**Table 2**  
Release rates of HRP from crosslinked anhydride networks

Formulation	24 h Burst (%)	Cumulative release after 48 h (%)	Long-term release (d7–d35) (%/d)	Cumulative release (%)
70:30 MCPH:MSA	3.81 ± 0.70	5.61 ± 0.78	0.05 ± 0.02	10.33 ± 0.89
70:30 MCPH:MSA + gelatin microparticles	15.22 ± 2.5	41.72 ± 17.3	0.518 ± 0.16	56.71 ± 18.6

manner this size range could not be evaluated to compare with the crosslinked gelatin system. Nevertheless, these HRP release studies showed that we can modulate the rate of release of active protein from our crosslinked anhydride system. Further enhancement in protein release can be achieved by varying the size, volume fraction or type of porogen.

### 3.2. HRP release from photocrosslinked PA matrices with gelatin microparticle-induced porosity: effect of loading and particle size

Since gelatin microparticles were better modulators of protein release than NaCl crystals, additional studies were pursued with gelatin microparticles alone. Initially, gelatin microparticles of two size ranges (180–250 and 250–300 μm) were incorporated into photocrosslinked PA networks at a loading of 75 v/v%, the maximal loading allowable (formulations described in Table 1b). Large microparticles were selected to maximize the effect in these proof-of-concept studies. HRP release profiles from these networks can be seen in Fig. 4. During the first 8 days of degradation and release, the release profiles were identical, regardless of microparticle size. After day 8, the rate of HRP release from samples containing 180–250 μm microparticles was  $0.48 \pm 0.11\%$  per day, while the rate of HRP release from samples containing 250–300 μm microparticles was  $1.22 \pm 0.06\%$  per day ( $p < 0.05$ ). Since larger (250–300 μm)

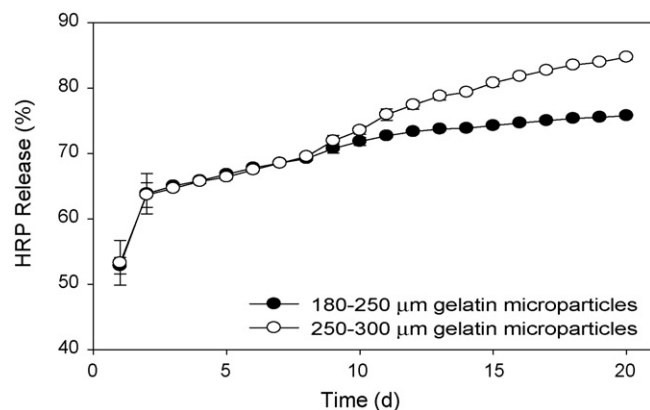


**Fig. 4.** Cumulative release kinetics of HRP from photocrosslinked anhydride networks containing gelatin microparticles into PBS at 37 °C with agitation (60 rpm). The cumulative normalized mass released from samples containing 75 v/v% gelatin microparticles, error bars represent mean ± S.D. for  $n = 2-4$ .

were often the result of the aggregation of smaller particles, additional studies utilized smaller, more uniform microparticles.

To evaluate the effect of gelatin microparticle size and loading on protein release, gelatin microparticles of two size ranges (106–180 and 180–250 μm) were utilized at loadings of 33 or 55 v/v%. Additionally, two MCPH:MSA ratios—30:70 and 70:30 were evaluated. These formulations are described in Table 1c. Interestingly, the release profile was independent of microparticle loading and MCPH:MSA ratio (Fig. 5). It is reasonable to postulate that the dissolution of the crosslinked gelatin microspheres albeit slow, would lead to the release of gelatin macromolecules, which upon diffusion and attainment of sufficient concentration would result in formation of fractal clusters that would lead to the formation of continuous aqueous channels. Based on percolation theory, such pathway formation would be favored if the size of the particles were larger as that would lead to a larger diffusion front and hence more rapid coalescence of these fronts leading to contiguous pathway formation. The larger microparticles (180–250 μm) yielded

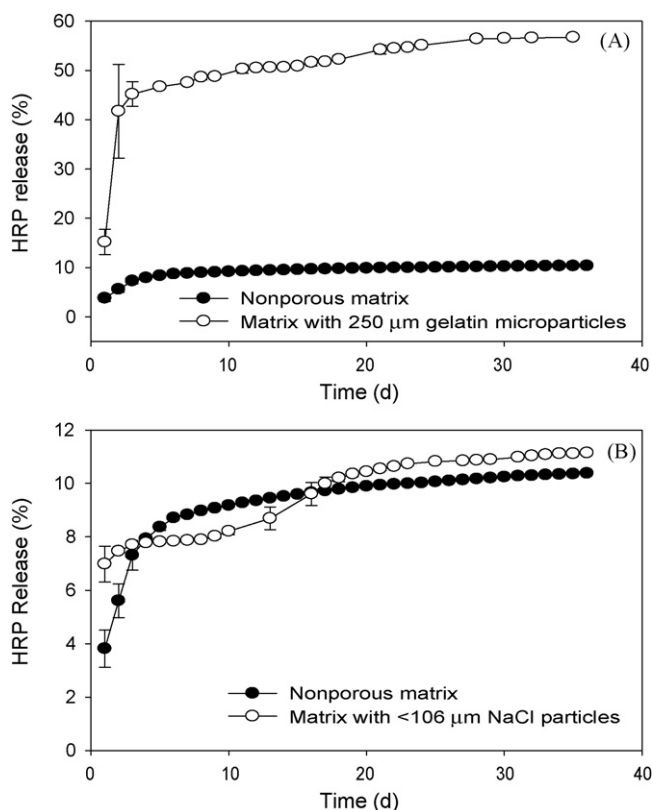


**Fig. 3.** Cumulative release kinetics of HRP from photocrosslinked anhydride networks containing gelatin microparticles (A) or NaCl particles (B) into PBS at 37 °C with agitation (60 rpm). Error bars represent mean ± S.D. for  $n = 2-4$ .

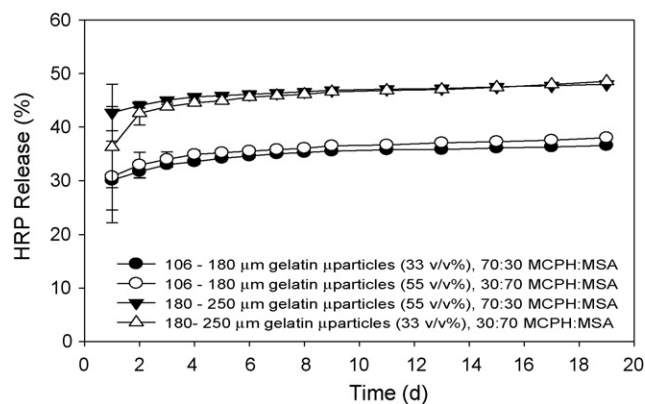


**Fig. 5.** Cumulative release kinetics of HRP from photocrosslinked anhydride networks containing gelatin microparticles into PBS at 37 °C with agitation (60 rpm). The cumulative normalized mass released from samples containing 106–180 or 180–250 μm gelatin microparticles, error bars represent mean ± S.D. for  $n = 4$ .

**Table 3**  
Experimental design for the evaluation of protein release from loaded gelatin microparticles and from photocrosslinked PA networks

Matrix	Granulated protein	Microparticle loading	Microparticle size ( $\mu\text{m}$ )	Protein loaded in microparticles
a				
N/A	N/A	N/A	106–180	FITC-BSA
N/A	N/A	N/A	106–180	HRP
N/A	N/A	N/A	180–250	HRP
b				
70:30 MCPH:MSA	HRP	10 w/w%	106–180	FITC-BSA
70:30 MCPH:MSA	FITC-BSA	10 w/w%	106–180	HRP

greater cumulative protein release than the smaller microparticles (106–180  $\mu\text{m}$ ) ( $p < 0.05$ ) regardless of MCPH:MSA ratio or microparticle loading percentage. This long-term release profile was primarily dominated by the release of HRP over the first 48 h.

### 3.3. Gelatin microparticles as protein delivery vehicles

Gelatin microparticles were also studied as a vehicle for protein delivery. Microparticles were loaded with a solution of FITC-BSA or HRP in PBS by swelling. Samples of loaded microparticles were then incubated in PBS release buffer. Combinations of protein type and microparticle size are described in Table 3a. The buffer was removed at predetermined time-points and protein release was quantified (Fig. 6). Microparticles (106–180  $\mu\text{m}$ ) loaded with FITC-BSA exhibited a 24-h burst release of  $59.98 \pm 0.79\%$  of loaded protein, while those loaded with HRP exhibited a smaller burst release of  $14.01 \pm 2.13\%$ . Larger microparticles (180–250  $\mu\text{m}$ ) loaded with HRP exhibited the smallest burst release ( $11.43 \pm 1.15\%$ ). Since the 180–250  $\mu\text{m}$  particles were less uniform than smaller microparticles (data not shown), these were not used to evaluate FITC-BSA release nor were they utilized in future studies. Final cumulative release was the greatest for FITC-BSA ( $93.49 \pm 2.2\%$  of loaded protein after 18 days). In contrast,  $81.64 \pm 0.07\%$  of loaded HRP was released from the 106–180  $\mu\text{m}$  microparticles and  $60.57 \pm 0.01\%$  of loaded HRP was released from 180–250  $\mu\text{m}$  microparticles. As expected, the total cumulative release of HRP was greater from the smaller microparticles, presumably a result of the increased surface area to volume ratio over the larger microparticles.

### 3.4. Dual release system for HRP and FITC-BSA from photocrosslinked PA matrix-gelatin microparticle composites

Composites of photocrosslinked PA networks and gelatin microparticles were fabricated to evaluate co-release of FITC-BSA

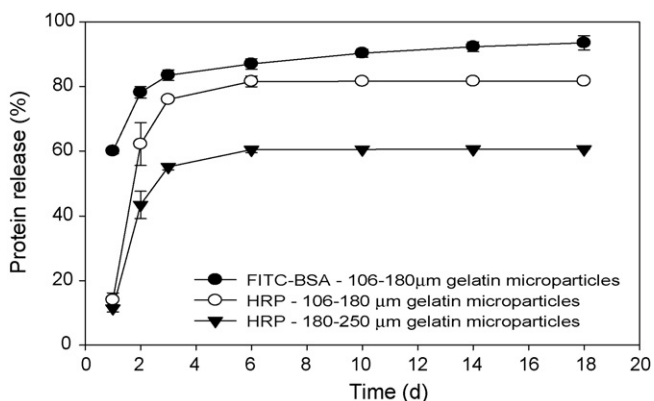


**Fig. 6.** Crosslinked gelatin microparticles were loaded with a solution of FITC-BSA or HRP; protein was released in 1 ml of PBS.

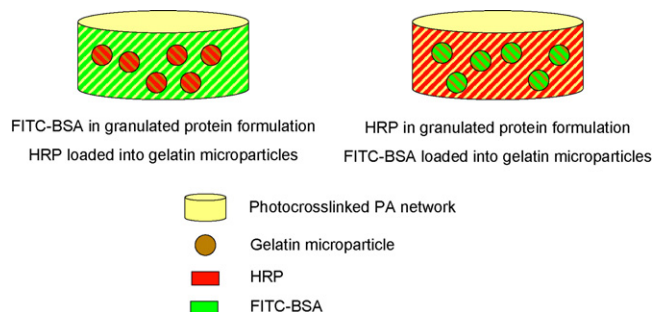


**Fig. 7.** Schematic for dual release strategy. Specimen contained HRP in the wet-granulated formulation and FITC-BSA-loaded gelatin microparticles or FITC-BSA in the wet-granulated formulation and HRP-loaded gelatin microparticles.

and HRP. One set of composites was created which contained FITC-BSA in the traditional wet granulated protein and cyclodextrin formulation and HRP-loaded gelatin microparticles. Another set of composites contained HRP in the traditional wet granulated protein and cyclodextrin formulation and FITC-BSA-loaded gelatin microparticles. A schematic for protein and microparticle loading is shown in Fig. 7. Release profiles were dependent on both the phase of protein loading (within gelatin microparticles or within the granulated formulation) and the type of protein (formulations described in Table 3b). When HRP was incorporated into composites in the granulated formulation with FITC-BSA-loaded gelatin microparticles (Fig. 8), there was a burst release of  $9.66 \pm 2.45\%$  of loaded HRP after 24 h. After 18 days, the cumulative release of HRP was  $11.20 \pm 0.002\%$  of the theoretical loading. Interestingly, only  $0.02 \pm 0.008\%$  of FITC-BSA from the composites was released after 18 days, with no detectable burst release. In contrast, when FITC-BSA

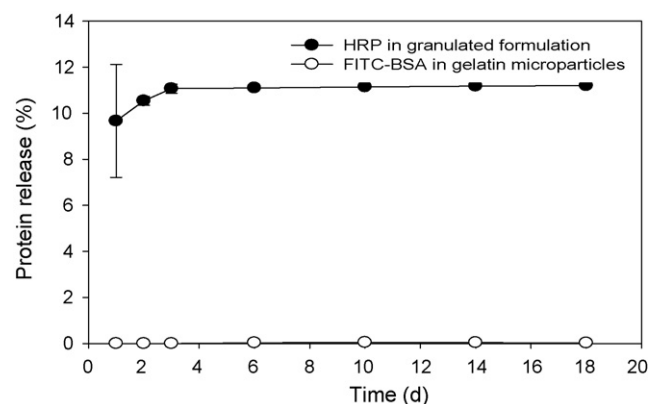


**Fig. 8.** Cumulative release kinetics of HRP and FITC-BSA from photocrosslinked anhydride networks containing gelatin microparticles into PBS at 37 °C with agitation (60 rpm). Samples contained traditionally formulated HRP (sugar + protein + granulation) (10 wt%) and FITC-BSA-loaded gelatin microparticles (10 wt%). The cumulative normalized mass released from samples is shown, error bars represent mean  $\pm$  S.D. for  $n = 2-4$ .

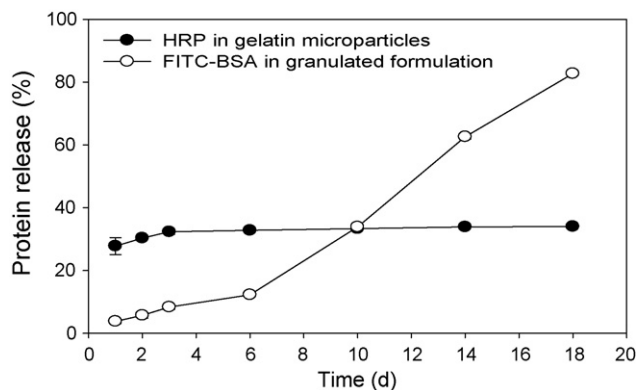


**Fig. 9.** Cumulative release kinetics of HRP and FITC-BSA from photocrosslinked anhydride networks containing gelatin microparticles into PBS at 37°C with agitation (60 rpm). Samples contained traditionally formulated FITC-BSA (sugar + protein + granulation) (10 wt%) and HRP-loaded gelatin microparticles (10 wt%). The cumulative normalized mass released from samples is shown, error bars represent mean  $\pm$  S.D. for  $n=2-4$ .

was incorporated into composites in the granulated formulation with HRP-loaded gelatin microparticles (Fig. 9), there was a burst release of  $5.73 \pm 0.87\%$  of loaded FITC-BSA after 24 h. After 18 days, the cumulative release of FITC-BSA was  $82.7 \pm 0.47\%$  of the theoretical loading. HRP release from gelatin microparticles within the composite yielded a burst release of  $30.32 \pm 0.19\%$ . Final cumulative release of HRP after 18 days was  $34.00 \pm 0.20\%$  of the theoretical loading.

#### 4. Discussion

Our laboratory has been the first to evaluate protein release from photocrosslinked PA networks (Weiner et al., 2008). This delivery system was initially selected as a result of numerous properties including the potential for predictable near-zero order release profiles, the capability of formation *in situ* by virtue of photocrosslinking, and the relative ease of system modification. In our initial study, sustained long-term release (>4 months) of macromolecules in their active form from photocrosslinked PA networks was demonstrated, although zero order release was not seen. Additionally, the release profiles of the evaluated macromolecules led to new conclusions regarding the mechanism of protein release from these networks. As expected, varying the network hydrophobicity (MCPH:MSA ratio or PEGDA content) altered the release profiles to achieve varying rates of protein release from the matrices. Surprisingly, these effects were seen primarily in the later phases (>7 days) of release. Interestingly, especially during the early phases of protein release, the physicochemical properties of individual proteins were a dominant factor in determining protein release.

If the mechanism for protein release were dictated purely by erosion of the polymer network, it would be expected that the release profile would be near-zero order and unrelated to physicochemical properties of the proteins. However, protein properties played a dominant role. The mechanism for protein release in the short-term appeared to be diffusion through matrix channels. As a result, release was dictated by protein properties (solubility and diffusivity) as well as by matrix properties (porosity and tortuosity). Protein-polymer interactions as dictated by both protein and matrix properties also assuredly play a critical role which cannot be measured by macroscopic experimentation. Also contributing to the theory that matrix porosity and protein properties were dominant factors in protein release was the observation that MCPH:MSA ratio, the main contributor to degradation rate, was not a good predictor of amount of protein release during the short-term. In

contrast, after roughly 7 days of release, network hydrophobicity and resulting degradation rate began to play the expected roles in modulating protein release.

In prior work, alteration of monomer ratios failed to achieve modulation of protein release in the short-term, therefore other avenues have been explored. Since porosity played a dominant role in dictating protein release, modifications in network porosity have been explored. Particulate leaching strategies are used in TE to induce porosity in scaffolds. In this process, leachable porogens such as salt or gelatin microparticles are incorporated uniformly into a scaffold. By incubation in aqueous buffer, the leachables are removed, leaving a uniformly porous scaffold. In the current study, the particulate leaching strategy was employed to fine tune protein release from photocrosslinked PA networks. Crosslinked gelatin microparticles (250  $\mu\text{m}$ ) or NaCl particles (<106  $\mu\text{m}$ ) were incorporated into photocrosslinked PA matrices of identical formulations. In specimen with gelatin microparticles, burst effect, long-term release rate, and total cumulative release rate of HRP were increased in comparison with unmodified networks (Fig. 3). However, in specimen containing NaCl particles, only burst release behavior was substantially increased. Although the crosslinked gelatin microparticles are slow to dissolve, the limited leaching of dissolved gelatin might leave an aqueous path, whereas the complete ionic dissolution of NaCl does not result in new aqueous pathways or macroporosity for protein diffusion and release. This theory may explain the difference in release for the two porogen types.

Particulate leaching of gelatin microparticles for facilitation of HRP release from photocrosslinked PA networks was further pursued. Initially, crosslinked gelatin microparticles of two sizes (180–250 or 250–300  $\mu\text{m}$ ) were incorporated into photocrosslinked PA networks at a loading of 75 v/v%. In this system, microparticle size played no role in the burst release or release rate during the first 8 days (Fig. 4). However, after 8 days, matrices with larger microparticles resulted in a higher rate of protein release. Since 75 v/v% was the upper limit for microparticle loading, and did result in some fracture during degradation, lower levels of loading were explored. A fractional factorial design of formulations was prepared with a high and low MCPH:MSA ratio (70:30 and 30:70), microparticle loading (55 and 33 v/v%) and gelatin microparticle size (180–250 and 106–180  $\mu\text{m}$ ). Interestingly, protein release was independent of both MCPH:MSA ratio and microparticle loading (Fig. 5). The larger gelatin microparticle size significantly increased cumulative protein release, although this was primarily a result of protein release during the initial 48 h. These data demonstrated that protein release can be modulated by a particulate leaching strategy. Regardless of gelatin microparticle size or loading, burst release and cumulative release were increased in comparison to nonporous matrices in previous studies. Experimental differences between the 75 v/v% loading and the lower (55 and 33 v/v%) loadings could be a result of a failure of the lower loadings to reach the percolation threshold for the material. This critical threshold concentration of porogens would result in an “infinite cluster” of conducting links, or pores through which the buffer can infiltrate (Romm, 2002). In this system, achieving the percolation threshold was not generally feasible; as structural integrity was compromised by high (75 v/v%) microparticle loading.

In addition to their usage in particulate leaching, gelatin microparticles have also been utilized for controlled delivery of growth factors as a result of ionic complexation capabilities (Yamamoto et al., 2001). In the current study, gelatin microparticles were loaded with protein solutions by partial swelling. During release, poorly associated protein was released into the release buffer during the initial 24 h as the microparticles reach equilibrium swelling (Fig. 6). FITC-BSA demonstrated a high burst

release from gelatin microparticles, yet also appeared to yield sustained release throughout the 18-day experimental conditions. HRP demonstrated less of a burst response than FITC-BSA; however, HRP release after 6 days was negligible. HRP release from smaller microparticles (106–180  $\mu\text{m}$ ) was greater than HRP release from larger microparticles (180–250  $\mu\text{m}$ ), presumably an effect of a higher surface area to volume ratio in the smaller microparticles. This difference in cumulative release was primarily dictated by HRP release between days 2 and 6.

Finally, further experiments examined the dual release of FITC-BSA and HRP from photocrosslinked PA network–gelatin microparticle composites. The goal of this dual release strategy was to create a system that could provide sustained release of two or more growth factors at different rates or release profiles. For example, in a system for tissue regeneration, a proliferative growth factor could undergo substantial release in the short-term, while a release of a differentiative growth factor could dominate in the long-term. In this study, protein-loaded microparticles were encapsulated into the photocrosslinked network along with a wet-granulated protein–cyclodextrin formulation. One composite formulation contained FITC-BSA-loaded gelatin microparticles and HRP in the wet-granulated phase (Fig. 8). The other composite formulation contained HRP-loaded gelatin microparticles and FITC-BSA in the wet-granulated phase (Fig. 9). The strategy of encapsulating drug- or protein-loaded microparticles in a matrix is commonly used to localize delivery to a specific site. In this system, the microparticles additionally confer porosity to the matrix to facilitate release of the protein in the wet-granulated phase.

When FITC-BSA was loaded into gelatin microparticles and HRP was present in the wet-granulated phase, surprisingly, there was no detectable release of FITC-BSA from the composite. Additionally, HRP release profiles were similar to profiles from a nonporous matrix. Alternatively, when HRP was loaded into gelatin microparticles and FITC-BSA was present in the wet-granulated phase, significant release of both HRP and FITC-BSA occurred. Release was greater than from nonporous matrices in previous studies. It was surprising that no appreciable release of FITC-BSA was detected from the composites containing FITC-BSA in the gelatin phase, although FITC-BSA does release from gelatin microparticles and HRP release from the matrix was observed. The phenomenon is presumably explained physicochemical properties of the proteins themselves.

## 5. Conclusions

This study details a means of modulating delivery of proteins from an injectable degradable system by incorporation of gelatin microparticles into the photocrosslinked PA system. Since protein diffusivity and matrix porosity in addition to matrix degradation were dominant factors in controlling protein release in previous studies, here we have focused on incorporation of porogens for increasing levels of protein release. When gelatin microparticles were included in matrices, microparticle size appeared to be the predominant factor affecting HRP release, with microparticle loading having no appreciable effect. Gelatin microparticles were also explored as a delivery vehicle. Both microparticle size and pro-

tein type (FITC-BSA or HRP) affected protein release from gelatin microparticles. By loading the protein in the gelatin microparticles, additional control over protein release was achieved. Furthermore, a dual release system has been demonstrated by incorporation of protein in both the PA matrix and the gelatin microparticles. Variation of system parameters – microparticle size, loading percentage, and protein loading of the microparticles – provide a versatile methodology for tailoring release profiles from photocrosslinked PA system. Future work will include further elucidation of the mechanisms of release, including porosity and aqueous channel formation.

## Acknowledgements

The authors are grateful for financial support from the Vanderbilt Institute for Integrative Biology and Education (VIIBRE) and from a Vanderbilt University Discovery Grant. They would also like to acknowledge support for AAW from the National Science Foundation Graduate Research Program.

## References

- Anseth, K.S., Shastri, V.R., Langer, R., 1999. Photopolymerizable degradable polyanhydrides with osteocompatibility. *Nat. Biotechnol.* 17, 156–159.
- Baroli, B., Shastri, V.P., Langer, R., 2003. A method to protect sensitive molecules from a light-induced polymerizing environment. *J. Pharm. Sci.* 92, 1186–1195.
- Burkoth, A.K., Burdick, J., Anseth, K.S., 2000. Surface and bulk modifications to photocrosslinked polyanhydrides to control degradation behavior. *J. Biomed. Mater. Res.* 51, 352–359.
- Determan, A.S., Trewyn, B.G., Lin, V.S., Nilsen-Hamilton, M., Narasimhan, B., 2004. Encapsulation, stabilization, and release of BSA-FITC from polyanhydride microspheres. *J. Control. Release* 100, 97–109.
- Draghi, L., Resta, S., Pirozzolo, M.G., Tanzi, M.C., 2005. Microspheres leaching for scaffold porosity control. *J. Mater. Sci. Mater. Med.* 16, 1093–1097.
- Hedberg, E.L., Kroese-Deutman, H.C., Shih, C.K., Crowther, R.S., Carney, D.H., Mikos, A.G., Jansen, J.A., 2005. Effect of varied release kinetics of the osteogenic thrombin peptide TP508 from biodegradable, polymeric scaffolds on bone formation in vivo. *J. Biomed. Mater. Res. A* 72A, 343–353.
- Holland, T.A., Tabata, Y., Mikos, A.G., 2005. Dual growth factor delivery from degradable oligo(poly(ethylene glycol) fumarate) hydrogel scaffolds for cartilage tissue engineering. *J. Control. Release* 101, 111–125.
- Liao, C.J., Chen, C.F., Chen, J.H., Chiang, S.F., Lin, Y.J., Chang, K.Y., 2002. Fabrication of porous biodegradable polymer scaffolds using a solvent merging/particulate leaching method. *J. Biomed. Mater. Res.* 59, 676–681.
- Muggli, D.S., Burkoth, A.K., Anseth, K.S., 1999. Crosslinked polyanhydrides for use in orthopedic applications: degradation behavior and mechanics. *J. Biomed. Mater. Res.* 46, 271–278.
- Muvaffak, A., Gurhan, I., Hasirci, N., 2004. Prolonged cytotoxic effect of colchicine released from biodegradable microspheres. *J. Biomed. Mater. Res. B Appl. Biomater.* 71, 295–304.
- Romm, F., 2002. Theories and theoretical models for percolation and permeability in multiphase systems: comparative analysis. *Adv. Colloid Interface Sci.* 99, 1–11.
- Saltzman, W.M., Langer, R., 1989. Transport rates of proteins in porous materials with known microgeometry. *Biophys. J.* 55, 163–171.
- Shastri, V.P., Marini, R.P., Padera, R.F., Kirchain, S., Tarcha, P., Langer, R., 1999. Osteocompatibility of photopolymerizable anhydride networks. *Mat. Res. Soc. Symp. Proc.* 530, 93–98.
- Tamada, J.A., Langer, R., 1993. Erosion kinetics of hydrolytically degradable polymers. *Proc. Natl. Acad. Sci. U.S.A.* 90, 552–556.
- Weiner, A.A., Gipson, M.E., Bock, E.A., Shastri, V.P., 2008. Photocrosslinked anhydride systems for long-term protein release. *Biomaterials* 29, 2400–2407.
- Weiner, A.A., Shuck, D.M., Bush, J.R., Shastri, V.P., 2007. In vitro degradation characteristics of photocrosslinked anhydride systems for bone augmentation applications. *Biomaterials* 28, 5259–5270.
- Yamamoto, M., Ikada, Y., Tabata, Y., 2001. Controlled release of growth factors based on biodegradation of gelatin hydrogel. *J. Biomater. Sci. Polym. Ed.* 12, 77–88.